Mechanics of Stochastic Fibrous Networks

A. M. SASTRY,* X. CHENG AND C. W. WANG
Department of Mechanical Engineering
and Applied Mechanics
University of Michigan
2250 G. G. Brown Building
2350 Hayward Street
Ann Arbor, MI 48109-2125

ABSTRACT: Point-bonded fibrous networks are used in a variety of engineering applications, including reinforcement for polymeric composites, paper, and electrochemical substrates, among many others. An understanding of the nature of the deformation of these irregular microstructures is key to developing useful manufacturing guidelines for their cost-effective production. The current approach allows such analysis, through use of a stochastic approach in constructing the network. Resulting network properties are compared with those in more regular arrays. Ultimately, determination of local deformations in these kinds of networks will be used to predict local deformation due to flow front progression in fibrous preforms for production of polymeric composite materials.

INTRODUCTION

VARIOUS APPROACHES HAVE been used in modeling of the deformation processes and effective stiffnesses of nonwovens and bonded nonwoven fibrous materials. The majority of classic approaches comprise conservation of strain energy analyses (e.g., Hearle and Newton, 1968; Hearle, 1980). These analyses revolve around calculation of the strain energy associated with affine deformations of unit cells of known orientation relative to the direction of applied load. The assumption of affine deformation, or deformation in which the strains at all scales of interest are geometrically similar, neglects effects such as microbuckling of fibers and random fiber slack. Other approaches (e.g., Backer and Petterson, 1960) employ averagings of orientation of fibers to derive the elastic moduli of bonded networks. While affine unit cell approaches and their extensions can provide

*Author to whom correspondence should be addressed.

0892-7057/98/03 0288-09 $10.00/0

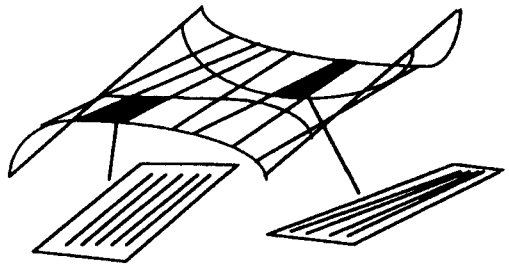

Figure 1. Local orientation can continuously vary in a preform using directed fiber techniques for preform production.

satisfactory prediction of elastic moduli of short fiber nonwovens, they amount to highly averaged, continuum predictions. Homogenization approaches (e.g., Gudes and Kikuchi, 1991) have also been developed to address the problem of optimization of structures using smoothed continuum constitutive rules calculated from known properties of distinct phases.

Current approaches in analysis of fibrous media can be thus categorized roughly into three types of models: (1) continuum approaches, relying upon macroscopic experiments to provide properties of interest, (2) micromechanical approaches using regular unit cells and constituent properties to model macroscopic properties (including both strength-of-materials approaches and elasticity approaches), and (3) homogenization approaches, where microstructural features are assessed and smoothed to produce local continuum properties.

Full optimization of these materials requires that models incorporate the specific microstructures obtainable, along with incorporation of their specified or anticipated statistical distributions in the component. Directed fiber approaches allow production of fibrous preforms, for example, Figure 1, with continuously varying fiber orientation, to within ±5° precision (e.g., Gerard and Jander, 1993).

Cost control in production of composites reinforced with these materials requires that analysis be detailed enough to (1) determine the effect of continuous changes in microstructure on these properties (e.g., the change in permeability with a 10% change in local orientation of fibers), and (2) determination of sensitivity to these properties to production specifications (e.g., the determination of angle sensitivity and fiber laydown and thus production precision).

Importantly, the connectivity of these microstructures greatly affects both processability and performance. Realistically, production parameters can be specified only as averages, with certain allowable variabilities. The cumulative distribution functions of all network parameters can be changed to produce simulated microstructures that can be studied using the current approach. The current approach employed stochastic microstructures for study of the material properties.

METHODOLOGY

Stochastic fiber networks were generated to understand and predict local deformations in point-bonded, fused fiber networks, addressing fundamental questions about the drapability and processability of these structures. The main approach involved four steps:

1. Networks were initially constructed by selecting distribution functions for six main variables: fiber volume fraction within a unit cell, fiber orientation distribution, fiber length distribution, fiber centerpoint (x- and y-) location, and fiber aspect ratio (L/d). Data were generated randomly according to these parameters, and fibers were "placed" in the unit cell, as in Figure 2(a). The intersection points were calculated and thereafter assumed to be rigid bonds.
2. Periodic boundary conditions were imposed [Figure 2(b)]. In this way, the initial volume fraction specified at the outset was imposed exactly for the unit cell, as ends were "wrapped" back into the cell. Also, periodic boundary conditions allowed analysis without spurious edge effects.
3. Non-load-bearing segments were removed. This included ends of overlapping fibers that did not intersect one of the load boundaries and structures within the cell that did not span the boundaries [Figure 2(c)], such as the triangle shown. Finally, a load direction was chosen (structures studied here were placed in uniaxial tension), and the networks were reduced accordingly, as in Figures 3(a) and 3(b), for x- and y-direction loading, respectively.

Using this methodology, several types of networks were constructed. By the technique described, the controllable parameters in the simulated networks were identical to those adjustable in a manufacturing process. The great majority of the generated structures were highly indeterminate (mechanisms, if bending were not considered to prevent unrestricted rotations about joints).

The analysis of the networks proceeded as follows. First, interfiber bonds were assumed to remain rigid and intact (Figure 4). Second, it was assumed that bonds were pointwise bonds. Third, bending was considered (Figure 4). In the uniaxial

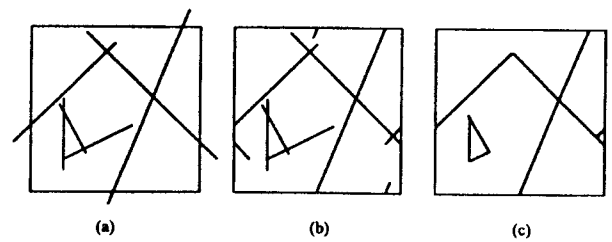

Figure 2. Network construction technique; square cells of unit area.

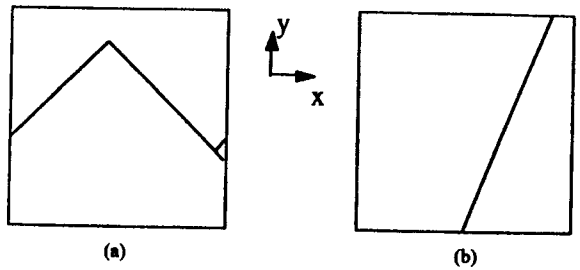

Figure 3. *Network [Figures 2(a)–(c)] reduced for x-loading [Figure 3(a)] and y-loading [Figure 3(b)] respectively.*

simulations described, a uniform displacement was applied at one edge, with the other edge fixed.

The mechanical analysis proceeds from a calculation of potential energy in the random structure (e.g., Cook et al., 1989). The general expression for potential energy in a linear elastic body is

$$\Pi_p = \int_v (1/2\{\varepsilon\}^T [E]\{\varepsilon\} - \{\varepsilon\}^T [E]\{\varepsilon_0\} + \{\varepsilon\}^T \{\sigma_0\})dV$$

$$- \int_v \{u\}^T \{F\}dV - \int_s \{u\}^T \{\Phi\}dS - \{D\}^T \{P\} \qquad (1)$$

where terms are defined

Π_p = potential energy
$\{u\}$ = displacement field
$\{\varepsilon\}$ = strain field
$[E]$ = stiffness matrix
$\{F\}$ = body forces
$\{\Phi\}$ = surface tractions
$\{D\}$ = nodal d.o.f. of the structure
$\{P\}$ = externally applied loads to d.o.f.
S, V = surface area, volume of structure
$\{\varepsilon_0\}$, $\{\sigma_0\}$ = initial values of $\{\varepsilon\}$, $\{\sigma\}$

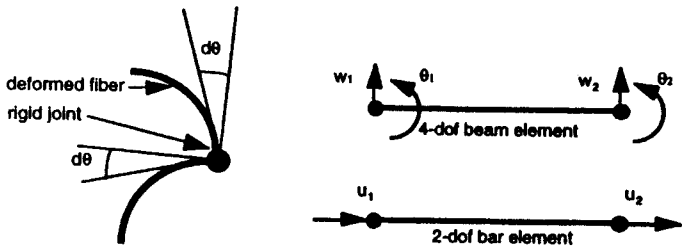

Figure 4. *Network loading scheme. Point bonds are assumed rigid; segment geometry can be altered through moment of inertia and aspect ratio.*

For a system of discrete elements (in this case, the segments between nodes), Equation (1) becomes

$$\Pi_p = 1/2 \sum_{n=1}^{numel} \{d\}_n^T [k]_n \{d\}_n - \sum_{n=1}^{numel} \{d\}_n^T \{r_3\}_n - \{D\}^T \{P\} \qquad (2)$$

where

$\{P\}$ = externally applied loads at nodes
$[k]$ = element stiffness
$[d]$ = transformation matrix (each "element" is oriented at a different angle)

Making Π_p stationary with respect to small changes in displacement, we obtain

$$[K]\{D\} = \{R\} \qquad (3)$$

where

$[K]$ = element stiffness
$\{D\}$ = nodal displacements; here, u, v, θ
$\{R\}$ = externally applied loads at nodes, here, at boundary nodes

A schematic of the deformation of fibers about a rigid bond is shown at left in Figure 4; the elements shown at right (uniform, and lying along the x-axis) were superposed to obtain the stiffness matrix:

$$[K'] = \int_0^L [B]^T EI[B]dx = \frac{AE}{L}\begin{bmatrix} 1 & 0 & 0 & -1 & 0 & 0 \\ 0 & 0 & 0 & 0 & 0 & 0 \\ 0 & 0 & 0 & 0 & 0 & 0 \\ -1 & 0 & 0 & 1 & 0 & 0 \\ 0 & 0 & 0 & 0 & 0 & 0 \\ 0 & 0 & 0 & 0 & 0 & 0 \end{bmatrix}$$

$$+ \frac{EI}{L^3}\begin{bmatrix} 0 & 0 & 0 & 0 & 0 & 0 \\ 0 & 12 & 6L & 0 & -12 & 6L \\ 0 & 6L & 4L^2 & 0 & -6L & 2L^2 \\ 0 & 0 & 0 & 0 & 0 & 0 \\ 0 & -12 & -6L & 0 & 12 & -6L \\ 0 & 6L & 2L^2 & 0 & -6L & 4L^2 \end{bmatrix} \qquad (4)$$

Table 1. Simulation parameters.

Case	Fiber Length	Fiber Aspect Ratio	Orientation Distribution
A	1	0.01	uniform, 0–90 degrees
B	1	0.02	uniform, 0–90 degrees
C	1	0.1	uniform, 0–90 degrees
D	1.5	0.01	uniform, 0–90 degrees
E	1.5	0.02	uniform, 0–90 degrees
F	1.5	0.1	uniform, 0–90 degrees

where (T) is the transformation matrix. Edge displacements (representing uniaxial tension for a displacement-controlled experiment) were applied to the boundary nodes of the cell. A unit dummy load technique was used to solve for the applied displacement boundary conditions.

Several cases were investigated to demonstrate the high variance in the behavior of these structures owing to their stochastic construction.

RESULTS

Table 1 summarizes the structures simulated. Five cases were studied to assess both the effect of bending on stochastic networks, as controlled by fiber aspect ratio (where higher aspect ratio fibers produce networks whose deformation is more bending-dominated), and the effect of fiber length-to-unit cell ratio on the networks (it was not the aim to determine a "percolation point," for short fiber materials, or a point at which the volume fraction was sufficiently high to produce a load-bearing network). Five networks were generated and reduced for each case. In case C, no load-bearing structures were generated for any of the five data (because of the high aspect ratio, the volume fractions studied dictated only between one and three fibers in each case); therefore, a plot is not included.

Several plots of normalized effective network modulus versus intial [Figure 2(b)] volume fraction are shown in Figures 5 and 6. A significant portion of the stochastic networks generated produced no load-bearing structures, resulting in zero normalized moduli.

DISCUSSION/FUTURE WORK

The nonaffine deformations within the structures produced moduli outside the bounds predictable by strength-of-materials approximations or by use of models for analysis of regular microstructures. The computed moduli in all cases, for example, were substantially less than those predicted via simple rule-of-mixtures, due to the significant role of bending in the deformation. Little difference was found in the structural properties of networks generated with staple lengths of 1–1.5.

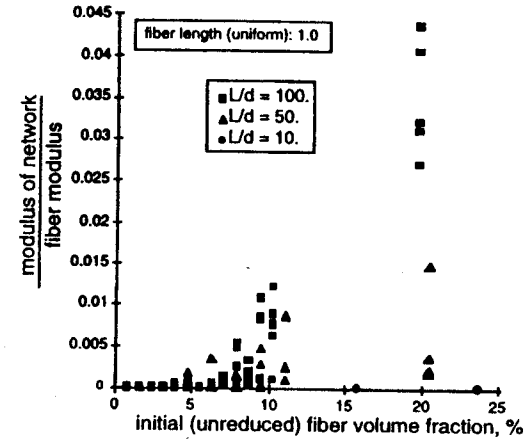

Figure 5. *Normalized network moduli, for fiber length = cell length.*

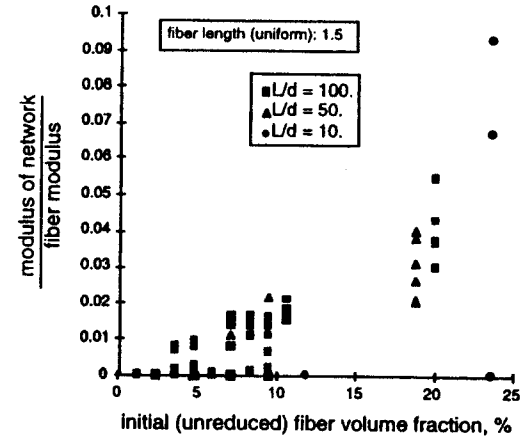

Figure 6. *Normalized network moduli, for fiber length = 1.5 cell length.*

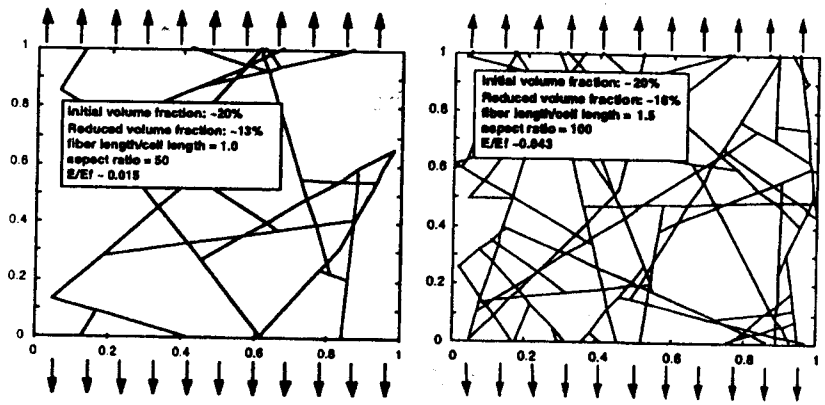

Figure 7. *Comparison of reduced networks generated for materials with aspect ratios of 50 (left) and 100 (right).*

Higher aspect ratio materials produced higher effective network moduli than lower aspect ratio materials, for the same initial volume fraction. This was due to the network connectivity (Figure 7): lower aspect ratio networks produced lower effective volume fractions than higher aspect ratio materials at the same initial volume fractions. These results suggest that an optimized process for mechanical properties may entail the use of higher aspect ratio fibers at low volume fractions for best connectivity in random structures.

Future work will include modeling of damage progression in these networks, due to a variety of load conditions. The effects of bond strength will also be considered, as will the effect of local architecture on flow front progression in liquid molding processes. Particularly, the effect of distributed loads on local network deformation will be of interest.

ACKNOWLEDGEMENTS

This work was supported in part by the Lawrence Berkeley Laboratories, through the Exploratory Research Program of the U.S. Department of Energy, Dr. Albert Landgrebe and Dr. Kim Kinoshita, program managers, and is gratefully acknowledged. Insightful technical discussions with Professor James R. Barber at the University of Michigan are also gratefully acknowledged.

REFERENCES

Backer, S. and D. R. Petterson. 1960. "Some Principles of Nonwoven Fabrics," *Textile Research Journal*, 30:704–711.

Cook, R. D., D. S. Malkus and M. E. Plesha. 1989. *Concepts and Applications of Finite Element Analysis*, John Wiley & Sons, New York.

Gerard, J. and M. Jander. February, 1993. *48th Annual Conference, The Composites Institute*, The SPI.

Gudes, J. M. and N. Kikuchi. 1990. "Preprocessing and Post Processing for Material Based on the Homogenization Method with Adaptive Finite Element Methods," *Computer Methods in Applied Mechanics and Engineering*, 83:143.

Hearle, J. W. S. 1980. "The Mechanics of Dense Fibre Assemblies," in *The Mechanics of Flexible Fibre Assemblies*, 51–86, J. W. S. Hearle, J. J. Thwaites and J. Amirbayat, eds., Sijthoff and Noordhoff, New York.

Hearle, J. W. S. and A. Newton. 1968. "Part XV: The Application of the Fiber Network Theory," *Textile Research Journal*, 1:343–351.